Mathematical models of magnetic circuits of high currents induction sensors for electric power supply systems devices of electric transport

S. Amirov, *K.* Turdibekov, *D.* Rustamov*, and *S.* Saydivaliev

Tashkent State Transport University, Tashkent, Uzbekistan

Abstract. The magnetic circuits of the developed high currents induction sensors for the electric power supply systems devices of electric transport are researched, analytical expressions of the magnetic flux in ferromagnetic connecting elements and magnetic voltage, the replacement circuit of the magnetic circuit elementary section, as well as mathematical models of the magnetic circuit of the developed sensors, are obtained.

1 Introduction

Currently, in the leading countries of the world, research work is being intensively carried out on the creation and development of monitoring sensors in electric transport power supply systems that provide high sensitivity, accuracy, and reliability of characteristics with great functionality.

But along with this, not enough attention has been paid to creating high current sensors that can be used to convert both direct and alternating with several output windings inductively disconnected between the sub for simultaneous connection to circuits for automatic metering of electrical energy, relay protection, and automation.

Nowadays, research works are being intensively carried out on the creation and development of monitoring sensors in electric transport power supply systems in the world's leading countries. Therefore, great importance is given to the research of induction sensors of high currents (ISHC), characterized by high sensitivity, accuracy, and reliability. To determine the characteristics of these sensors, it is necessary to research and develop their mathematical models. The electromagnetic circuit of the developed induction sensors of high currents (ISHC) is a circuit with distributed electrical and magnetic parameters [1-8]. These parameters include the linear values of the magnetic resistance of C-shaped ferromagnetic concentric rings, the magnetic capacitances of the gap between these rings and the longitudinal ampere-turns per unit of the angle of the magnetic circuit, the linear values of the magnetic resistance of the connecting ferromagnetic elements, the magnetic capacitances of the gap between these connecting elements and the longitudinal ampere-turns of the modulation winding, per unit the lengths of these connecting elements.

*Corresponding author: rustamov_d1976@mail.ru

The main factors are the change in magnetic voltage and magnetic flux along the length of the magnetic circuit in induction sensors with distributed parameters, particularly in the developed ISHC [9-12].

It is necessary to develop their mathematical models considering the distribution of the electromagnetic parameters of the circuits and the nonlinearity of the main magnetization curve of the ferromagnetic material for the theoretical research of the new ISHC electromagnetic circuits and their main characteristics.

These models are based on analytical expressions of magnetic flux and magnetic voltage as a function of the location coordinates of the windings.

2 Methods

The theory of electric circuits with distributed parameters, the theory of the electromagnetic field, and experimental research methods, are used.

These models are based on analytical expressions of magnetic flux and magnetic voltage as a function of the location coordinates of the windings

The modulation magnetic circuits of the developed ISHC [2, 13, 14, 15, 16] consist of two C–shaped parallel sections with cutouts (a rod pair form) along the profile, interconnected by two ferromagnetic connecting elements made with rectangular cutouts (a rod pair form) and modulating windings arranged evenly on each rod pair of C–shaped sections and the connecting element (fig. 1).

Each section of C-shaped magnetic circuits with corresponding modulating windings and a connecting element with modulating windings represent a separate magnetic circuit, practically magnetically unrelated to each other. The conditions for creating a magnetic field are almost the same in all three magneto modulation circuits: the modulating magnetic field is created by magnetizing windings evenly distributed along parallel rods.

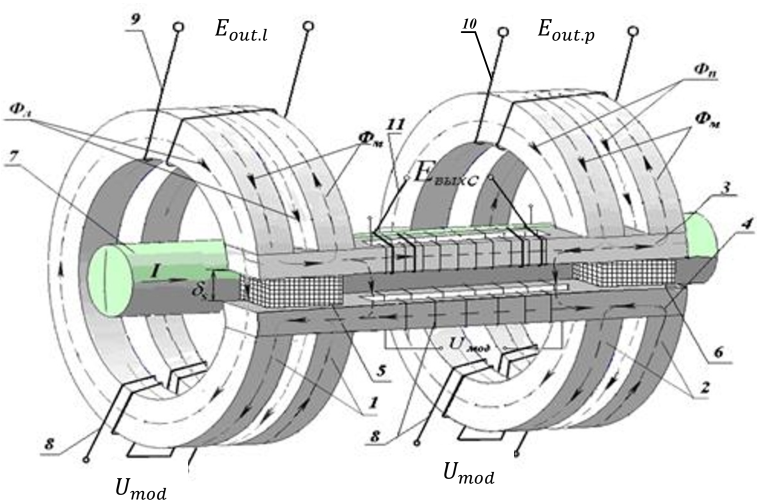

Fig. 1. Design diagram of the developed device for converting current into voltage with wide functionality: 1 and 2 are C is shaped parallel sections of the magnetic circuit with cutouts, 3 and 4 are ferromagnetic connecting elements, 5 and 6 are wedges, 7 is conductive bus, 8 is modulating windings, 9, 10, 11 are three measuring (output) windings

The magnetic flux of the converted current in C-shaped sections of a magnetic circuit is determined based on Ohm's law as:

$$Q_{\mu x}^{c} = \frac{F_x}{\Sigma z_\mu} = \frac{I_x w_x}{z_{\mu 0} + z_{\mu\delta}}, \quad (1)$$

where $Z_{\mu 0} = \frac{2\pi r_{cp} \alpha_m}{\mu\mu_0 (r_{\text{н}} - r_{\text{в}}) h_1 360^0}$, $Z_{\mu 0} = \frac{\delta_{\text{p}}}{\mu_0 b_P X_m}$ is magnetic resistances, respectively, of the C-shaped magnetic core and the air gap in the path of the magnetic flux $Q_{\mu x}^{c}$.

If we take into account that $\mu >> 1$ and, therefore $Z_{\mu\text{ст}} << Z_{\mu\delta}$, then equation (1) in the first approximation can be rewritten in the following form:

$$Q_{\mu x}^{c} \approx \frac{F_x}{z_{\mu\delta}}. \quad (2)$$

Magnetic induction in one section of C - shaped magnetic conductors is as:

$$B_{\text{ст}}^{c} = \frac{Q_{\mu x}^{c}}{2 b_2 h_2}. \quad (3)$$

The converted current magnetic field strength magnitude in a C-shaped magnetic circuit is determined as follows:

$$\text{H}_x^c = \frac{B_{\text{ст}}^c}{\mu_0}. \quad (4)$$

We find analytical expressions of the magnetic flux in ferromagnetic connecting elements and the magnetic voltage between them along the length of these elements created by the converted current I_x (Fig. 2). We calculate this magnetic circuit by superposition, i.e., first, we determine the partial values of magnetic fluxes and voltages created separately from the left and right sources of the magnetomotive force (MMF) F_x, and then we find their common values by algebraic summation [3]. The replacement scheme of the elementary section of the magnetic section of the magnetic circuit of the converted current is shown in Fig. 3.

Differential equations compiled based on Kirchhoff's laws for an elementary section of a magnetic circuit *dx* have the following form:

$$Q_{\mu x}^{L} - U_{\mu x}^{L} \text{C}_{\mu p} dx - Q_{\mu x}^{L} - dQ_{\mu x}^{L} = 0$$

or

$$\frac{dQ_{\mu x}^{L}}{dx} = -U_{\mu x}^{L} \text{C}_{\mu p}, \quad (5)$$

$$-U_{\mu x}^{L} + Q_{\mu x}^{L} dx + U_{\mu x}^{L} + dU_{\mu x}^{L} + Z_{\mu p} Q_{\mu x}^{L} dx = 0$$

or

$$\frac{dU_{\mu x}^{L}}{dx} = -2 Z_{\mu x} Q_{\mu x}^{L}, \quad (6)$$

where $Q_{\mu x}^{L}, U_{\mu x}^{L}$ are accordingly, the magnetic flux and magnetic voltage generated by the MMF source of the left section of C - shaped magnetic circuits with a converted current I_x, i.e. $F_x = I_x w_x$; $Z_{\mu\text{p3}} = \frac{1}{2\mu\mu_0 b_2 h_2}$, $C_{\mu\text{p3}} = \mu_0 \frac{2 b_2}{\delta_p}$ is linear values of the magnetic resistance of parallel rods of ferromagnetic connecting elements and the magnetic capacitance between them per unit length *x*.

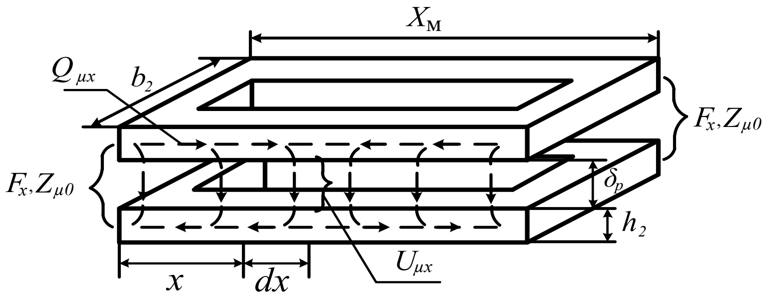

Fig. 2. Magnetic circuit of a ferromagnetic connecting element with a converted current

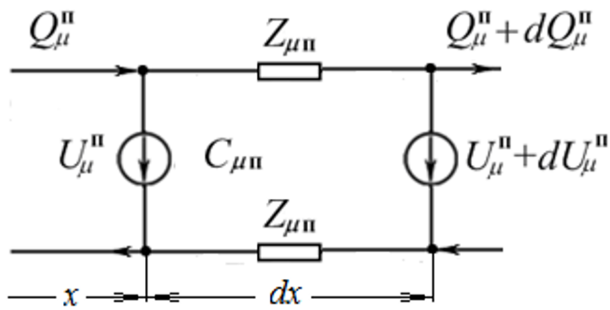

Fig. 3. Replacement scheme of the magnetic circuit elementary section of a ferromagnetic connecting element with a converted current

Differentiating (6) and substituting (5) into it, we obtain the following second-order differential equation:

$$\frac{d^2U_{\mu x}^L}{dx^2} = 2Z_{\mu p3}C_{\mu p3}U_{\mu x}^L. \quad (7)$$

The general solution of this differential equation, according to [4], has the following form:

$$U_{\mu x}^L = A_1e^{\gamma 3x} + A_1e^{-\gamma 3x} \quad (8)$$

where $\gamma_3 = \sqrt{2Z_{\mu p3}C_{\mu p3}}$ is the propagation coefficient of the magnetic flux in the magnetic circuit; A_1, A_2 are constant integrations.

Differentiating (8) and substituting it into (6), we find the expressions of the magnetic flux:

$$U_{\mu x}^L = -\frac{\gamma_3 A_1}{2Z_{\mu p3}}e^{\gamma 3x} + \frac{\gamma_3 A_2}{2Z_{\mu p3}}e^{-\gamma 3x}. \quad (9)$$

The constant integrations A_1 and A_2 are determined from the following boundary conditions:

$$U_{\mu x}^L = |x = 0 = F_x - Q_{\mu x}^L\big|_{x=0} \cdot Z_{\mu 0}, \quad (10)$$

$$U_{\mu x}^{L} = \left| x = X_m = Q_{\mu x}^{L} \right|_{x=\mathrm{X}_m} \cdot Z_{\mu\mathrm{T}}. \quad (11)$$

where $Z_{\mu p,}$ is the magnetic resistance of the left section of C-shaped magnetic cores; $Z_{\mu\mathrm{T},}$ is the magnetic resistance of the forming surfaces of the right section of C-shaped magnetic cores.

Substituting the values of the magnetic flux and magnetic voltage at $\mathrm{x} = 0$ and $\mathrm{x} = \mathrm{X}_m$ following (8) and (9) in (10) and (11), we obtain the following system of algebraic equations:

$$\begin{cases} \left(1-\frac{y_3 Z_{\mu 0}}{2Z_{\mu p3}}\right)\mathrm{A}_1+\left(1-\frac{y_3 Z_{\mu 0}}{2Z_{\mu p3}}\right)\mathrm{A}_2=F_x \\ \left(1+\frac{y_3 Z_{\mu\mathrm{T}}}{2Z_{\mu p3}}\right)e^{\gamma_3 X_M}A_1+\left(1-\frac{y_3 Z_{\mu\mathrm{T}}}{2Z_{\mu p3}}\right)e^{-\gamma_3 X_M}A_2=0 \end{cases} \quad (12)$$

$$\begin{cases} \left(1-\frac{y_3 Z_{\mu 0}}{2Z_{\mu p3}}\right)\mathrm{A}_1+\left(1+\frac{y_3 Z_{\mu 0}}{2Z_{\mu p3}}\right)\mathrm{A}_2=F_x \\ \left(1+\frac{y_3 Z_{\mu\mathrm{T}}}{2Z_{\mu p3}}\right)e^{\gamma_3 X_M}A_1+\left(1-\frac{y_3 Z_{\mu\mathrm{T}}}{2Z_{\mu p3}}\right)e^{-\gamma_3 X_M}A_2=0 \end{cases} \quad (13)$$

Solving equations (12) and (13) together concerning A_1 and A_2, we have:

$$A_1 = -\frac{F_x}{2\Delta}e^{-y_3 X_M} + \frac{F_x \gamma_3 Z_{\mu\mathrm{T}}}{4\Delta_4 Z_{\mu P_3}}\mathrm{e}^{-\gamma_3 \mathrm{X}_M} \quad (14)$$

$$A_2 = -\frac{F_x}{2\Delta}e^{-y_3 X_M} + \frac{F_x \gamma_3 Z_{\mu\mathrm{T}}}{4\Delta_4 Z_{\mu p3}}\mathrm{e}^{-\gamma_3 \mathrm{X}_M} \quad (15)$$

where $\Delta_4 = \left(1 + \frac{{y_3}^2 Z_{\mu 0} Z_{\mu T}}{4Z^2{}_{\mu p3}}\right) sh\beta_3 + \frac{{y_3}^2 Z_{\mu 0} Z_{\mu T}}{4Z^2{}_{\mu p3}} ch\beta_3$

Taking into account (14) and (15), equations (7) and (8) take the following form:

$$U_{\mu\mathrm{x}}^{L} = \frac{F_x}{\Delta_4}\{sh[\gamma_3(X_M - \mathrm{x}] + \frac{y_3 \quad Z_{\mu T}}{2Z \quad {}_{\mu p3}} ch[\gamma_3(X_M - \mathrm{x})]\} \quad (16)$$

$$Q_{\mu\mathrm{x}}^{L} = \frac{\gamma_3 F_x}{2\Delta_4 Z_{\mu p3}}\{ch[\gamma_3(X_M - \mathrm{x}] + \frac{y_3 Z_{\mu T}}{2Z_{\mu p3}} ch[\gamma_3(X_M - \mathrm{x})]\}. \quad (17)$$

The expressions for the magnetic voltage and magnetic flux generated only by the MMF of the right section of the C-shaped magnetic conductors are similar. Here we confine ourselves to giving their final expressions, i.e.:

$$U_{\mu\mathrm{x}}^{L} = \frac{F_x}{\Delta_4} sh(\gamma_3 \mathrm{x}) + F_\mathrm{x}\frac{y_3 Z_{\mu T}}{2Z_{\mu p3}\Delta_4} ch(\gamma_3 \mathrm{x}) \quad (18)$$

$$Q_{\mu\mathrm{x}}^{L} = \frac{\gamma_3 F_x}{2Z_{\mu p3}\Delta_4} ch(\gamma_3 \mathrm{x}) + F_x \frac{y_3 Z_{\mu T}}{2Z^2{}_{\mu p3}\Delta_4} sh(\gamma_3 x) \quad (19)$$

Expressions for the total magnetic stresses and magnetic fluxes generated by both sources of MMF are found by algebraic summation of their particular values, i.e.:

$$U_{\mu\mathrm{x}} = U_{\mu x}^{L} + U_{\mu x}^{p} = \frac{F_x}{\Delta_4}\{sh[\gamma_3(X_M - \mathrm{x}] + sh(\gamma_3 x) + \frac{y_3 Z_{\mu T}}{2Z_{\mu p3}\Delta_4} \cdot ch(\gamma_3 \mathrm{x})\{ch[\gamma_3(X - x)] + ch(\gamma_3 x)\}\} \quad (20)$$

$$Q_{\mu\mathrm{x}} = Q_{\mu x}^{L} + Q_{\mu x}^{p} = \frac{\gamma F_x}{2Z_{\mu p3}\Delta_4}\{ch[\gamma_3(X_M - \mathrm{x}] - ch(\gamma_3 x) + \frac{y_3 Z_{\mu T}}{2Z_{\mu p}} sh[\gamma_3(X - x)] - sh(\gamma_3 x)\}\} \quad (21)$$

Expressions (20) and (21) will be simplified if, in the first approximation, we assume that $Z_{\mu\text{т}} \to \infty$, i.e. $Q_\mu^L\big|_{x=X_M} = 0$ and $Q_\mu^P\big|_{x=X=0} = 0$. Then, taking into account these assumptions, expressions (20) and (21) will have the following form:

$$U_{\mu x} = \frac{F_x}{\Delta_5}\{ch[\gamma_3(X_m - x)] + ch(\gamma_3 x)\}, \quad (22)$$

$$U_{\mu x} = \frac{\gamma_3 F_x}{2Z_{\mu\text{р}3}\Delta_5}\{sh[\gamma_3(X_m - x)] - sh(\gamma_3 x)\}, \quad (23)$$

where $\Delta_5 = ch(\gamma_3 X_m) + \frac{\gamma_3 Z_{\mu 0}}{2Z_{\mu\text{р}3}} sh(\gamma_3 X_m)$.

Using the well-known hyperbolic trigonometry formulas, we obtain the following expressions, which are more convenient for the analysis and calculation of magnetic circuits:

$$U_{\mu x} = F_x \frac{2ch\left(\frac{1}{2}\beta_3\right)}{\Delta_5} ch\left[\beta_3\left(\frac{1}{2} - x*\right)\right], \quad (24)$$

$$Q_{\mu x} = F_x \frac{\beta_3 ch\left(\frac{1}{2}\beta_3\right)}{Z_{\mu 3}\Delta_5} sh\left[\beta_3\left(\frac{1}{2} - x*\right)\right], \quad (25)$$

where β_3 is the magnetic attenuation coefficient and equal to $\gamma_3 X_m$.

Figures 4 and 5 show the curves of dependence $U_\mu^* = f(x*)$ and $Q_\mu^* = f(x*)$ at different values ofβ_3, where $U_{\mu x}^* = \frac{U_{\mu x}}{U_{\mu x}|x=0}$, ⇄ $Q_{\mu x}^* = \frac{U_{\mu x}}{U_{\mu x}|x=0}$ and $x* = \frac{x}{X_m}$.

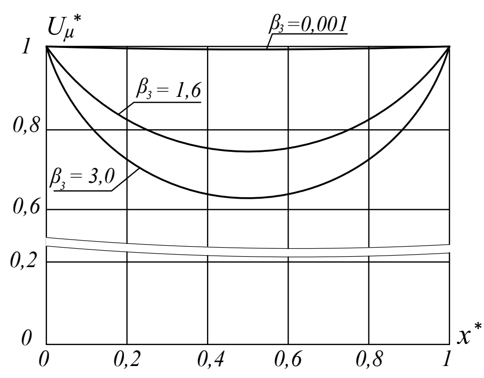

Fig. 4. The curves of dependence $U_{\mu x}^*(x*)$ at different values of β_3

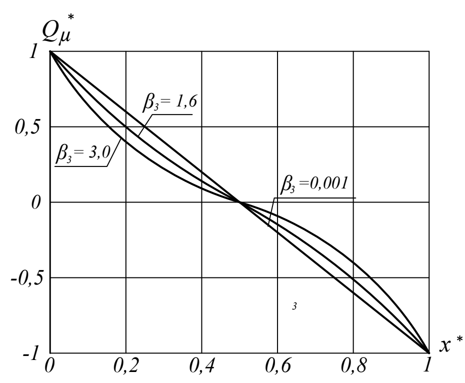

Fig. 5. The curves of dependence $U_{\mu x}^*(x*)$ at different values of β_3

The obtained expressions (24) and (25) analysis of the magnetic circuit of ferromagnetic connecting elements with the converted current of the developed ISHC and their curves in relative units shows that the magnetic voltage along the magnetic circuit is unstable and has a minimum value at the magnetic neutral point, and the magnetic flux is distributed non-linearly and changes its sign at the magnetic neutral point, moreover, with an increase in the attenuation coefficient of the magnetic flux β_3, the variability of the magnetic voltage and the degree of nonlinearity of the distribution of the magnetic flux along the length of the magnetic circuit, it increases.

The modulating magnetic field strengths in the corresponding sections of the ferromagnetic connecting element are as follows:

$$\mathrm{H}_m(\mathrm{x}_1) = \frac{1}{0{,}5\mathrm{X}_m} Z_{\mu\text{p}2} \int_0^{0{,}5\mathrm{X}_m} Q_\mu(\mathrm{x}_1) dx_1 = f_{m2}\left[1 - \frac{k_{\text{т}2}}{\Delta_3} sh(0{,}5X_m)\right] \quad (26)$$

$$\mathrm{H}_m(\mathrm{x}_2) = \frac{1}{0{,}5\mathrm{X}_m} Z_{\mu\text{p}2} \int_0^{0{,}5\mathrm{X}_m} Q_\mu(\mathrm{x}_2) dx_2 = f_{m2}\left[1 - \frac{k_{\text{т}2}}{\Delta_3} sh(0{,}5X_m)\right] \quad (27)$$

Expressions (26) and (27) are mathematical models of magnetic circuits with modulating windings of a ferromagnetic connecting element developed by ISHC.

3 Results and discussion

Thus, the method of calculating the nonlinear magnetic circuits of the developed sensor for converting direct and alternating current into voltages with advanced functionality has been improved. The results of this study have been tested at scientific and practical conferences.

4 Conclusions

1. It is revealed that high current sensors must have advanced functionality, high sensitivity, accuracy, and linearity of converting high currents into an electrical signal, as well as stability and characteristics under extreme operating conditions.
2. Improved calculation of nonlinear magnetic circuits with distributed electrical and magnetic parameters.
3. Mathematical models of induction sensors of high currents have been developed.
4. High-current induction sensors have been developed for electric transport power supply systems.

References

1. Amirov S.F., Safarov A.M., Rustamov D.S. Electromagnetic current sensor for control systems of traction power supply devices. Chemical technology. Control and management. No. 2. pp. 26-31. (2014).
2. Amirov S.F., Safarov A.M., Turdybekov K.H., Rustamov D.S., Khushbokov B.H. Patent of the Republic of Uzbekistan No. 04217. Device for current conversion. Official Bulletin, No. 8. (2010).
3. Tumanski S. Principles of electrical measurement. CRC press. (2006).
4. Zaripov M. F., and Petrova I. Y. Energy-informational method of analysis and synthesis of sensitive elements of control systems, Datch. (1999).
5. Mocevic, S., Wang, J., Burgos, R., Boroyevich, D., Jaksic, M., Stancu, C., & Peaslee, B. Comparison and discussion on shortcircuit protections for silicon-carbide MOSFET modules: Desaturation versus Rogowski switch-current sensor. IEEE Transactions on Industry Applications, 56(3), 2880-2893. (2020).
6. Amirov, S., Rustamov, D., Yuldashev, N., Mamadaliev, U., & Kurbanova, M. Study on the Electromagnetic current sensor for traction electro supply devices control systems. In IOP Conference Series: Earth and Environmental Science,Vol. 939, No. 1, p. 012009. (2021).
7. Khomenko, B. I., & Suslova, K. N. Unified converter for electric locomotives of direct and alternating current. Russian Electrical Engineering, 80(6), 318-322. (2009).

8. Volokhin V., & Diahovchenko, I. Peculiarities of current sensors used in contemporary electric energy metering devices. Energetika, 63(1). (2017).
9. Gurtovtsev A.L. Measuring current transformers for 0.4 - 10 kV. Possibilities of improving the characteristics. Electrical Engineering News. № 1(49). pp. 46-54. (2008).
10. Appolsky S.M., Gorsky A.N. Calculations of electromagnetic fields. Moscow, (2006).
11. Artenyev B.G. Verification and calibration of measuring instruments. p. 406 (2006).
12. Atamalyan E.G. Devices and methods for measuring electrical quantities. (2005).
13. Turdibekov, K., Yakubov, M., Sulliev, A., & Sanbetova, A. Mathematical Models of Asymmetric Modes in High-Speed Traffic. In XIV International Scientific Conference "Interagromash 2021" Precision Agriculture and Agricultural Machinery Industry, Vol. 2, pp. 1051-1058. Cham: Springer International Publishing. (2021).
14. Amirov, S., Rustamov, D., Yuldashev, N., Mamadaliev, U., & Kurbanova, M. Study on the Electromagnetic current sensor for traction electro supply devices control systems. In IOP Conference Series: Earth and Environmental Science, Vol. 939, No. 1, p. 012009. (2021).
15. Rustamov D.Sh. Application of the method of parametric structural diagrams to determine the error of electromagnetic converters of high currents. International scientific and technical conference "Actual problems of the power supply system". pp. 214-216. (2021).
16. Safarov A.M., Rustamov D.Sh. Comparative analysis of modern current transformers in traction power supply system and future development. Problems of energy and resource saving. Vol. 6, (2021).